

Defect chemistry of donor-doped BaTiO₃ with BaO-excess for reduction resistant PTCR thermistor applications - redox-behaviour

Christian Pithan,^{*a} Hayato Katsu^b and Rainer Waser^{ac}

Received 00th January 20xx,
Accepted 00th January 20xx

DOI: 10.1039/x0xx00000x

www.rsc.org/

The electric conductivity of donor-doped BaTiO₃ thermistor ceramics with excessive BaO revealing a reduction-persistent PTCR effect has been carefully examined in dependence of materials composition and oxygen partial pressure at moderate temperatures between 973 and 1273 K. This thermal regime represents the range which is relevant for the realization of insulating grain boundaries in these electrically inhomogeneous ceramic materials through reoxidation. Based on the experimental results strong evidence for a general correlation between the PTCR characteristics, DC-conductivity and the herewith associated defect chemistry significant to thermistor applications is presented for the system (Ba, La)_mTiO₃, where *m* designates the BaO-excess (*m* ≥ 1). Nominal compositions with a relatively low (Ba+La)/Ti ratio *m* only show a rather poor PTCR effect and an overall donor-type response in conductivity can be observed at all levels of oxygen partial pressure considered in the present study. With increasing (Ba+La)/Ti ratio *m* the nonlinear resistivity jump with raising temperature strongly improves and acceptor-type behaviour seems to dominate the total conductivity at partial pressures of oxygen above approximately 10⁻⁶ MPa. This result for compositions with high BaO-excess can be understood by the local formation of point defect associates in the grain boundary regions that consist of both acceptor-type titanium vacancies and donor-type oxygen vacancies. Their origin is attributed to the preferential local incorporation of excessive BaO into the BaTiO₃ lattice at the intergranular interfaces.

1. Introduction

The ferroelectric perovskite compound BaTiO₃ has been technically utilized in a variety of electroceramic applications since its discovery.¹ One of them are resistors with positive temperature coefficient of resistivity (PTCR) which are employed for surge current limitation in electronic circuitry, self-regulated heating and for resettable fuses, just to mention a few examples.²⁻⁴ Commonly these passive electronic components are referred to as thermistors. Due to economic reasons, the overall electric resistance is generally required to be as low as possible during the stationary state of use in order to reduce unnecessary power losses. For this purpose, recently, devices with a multi-layered structure composed of consecutive ceramic layers of donor-doped BaTiO₃ with alternating inner metallic electrodes on Ni-basis have been introduced.⁵ Since all resistive ceramic layers are connected in parallel in this arrangement the total resistance of the whole device is efficiently decreased.

Likewise to BaTiO₃-based chip type PTCR-devices also the multi-layered counterparts show a drastic enhancement in resistivity up to several orders of magnitude upon heating. This resistivity jump occurs when the temperature reaches and surpasses the phase transition point of the ceramic phase, the so-called Curie Temperature *T_C*, where the ferroelectric modification of barium titanate transforms into the paraelectric polymorph. The physical phenomenon responsible for this resistivity increase is commonly referred to as the PTCR-effect^{6,7} and only occurs in polycrystalline systems such as sintered ceramics.⁸

It has been believed for a long time that BaTiO₃-based PTCR materials must be sintered under oxidizing conditions. Daniels et al.⁹ showed that oxidized, electrically insulating grain boundary layers separating the semiconducting cores of the donor-doped grains are responsible for the generation of the PTCR-effect. According to their point defect chemical analysis based on measurements of high temperature DC-conductivity¹⁰, the formation of metal vacancies compensates positively charged donor impurities during local reoxidation of the intragranular interfaces. This mechanism takes place more favourably than compensation by electrons, a process that is prevailing only in the interior of the grains and not at the grain boundaries. This conception has been confirmed later by thermogravimetric studies.¹¹ In consequence the local enrichment of immobile and negatively charged acceptor states created by metal vacancies at the grain boundaries gives rise to resistive back-to-back Schottky type barriers.

^aInstitute for Electronic Materials, Peter Grünberg Institute, Forschungszentrum Jülich GmbH, 52428 Jülich, Germany & Jülich Aachen Research Alliance for Fundamentals on Future Information Technology (JARA-FIT)

^bMurata Manufacturing Corporation Limited, 1-10-1 Higashi-kotari, Nagaokakyo-shi, Kyoto, 617-8555 Japan

^cInstitute for Electronic Materials II, Rheinisch-Westfälische Technische Hochschule Aachen, Sommerfeldstraße 24, 52074 Aachen, Germany

They impede the motion of electrons from one grain into a neighbouring one, if the space charges arising from ferroelectric polarization do not counterbalance their electrostatic potential, which is actually the case for paraelectric BaTiO₃, i.e. above T_C .⁷ In the view of this defect chemical scenario a demanding technological challenge has been to develop reduction resistant ceramic formulations for multilayer PTCR-components that preferentially should contain Ni-based metallic alloys as electrode material. In this case, the metallic and ceramic material must be cofired under reducing conditions in order to avoid excessive oxidation and corrosion of the metallic electrodes. On the other hand, from the defect chemical point of view, the generation of the PTCR effect requires a local oxidation of the grain boundaries in BaTiO₃.

In the recent past, newly developed rare-earth metal doped BaTiO₃-based ceramic PTCR formulations with excessive BaO, that can be sintered under reducing conditions at an oxygen partial pressure of oxygen of 10⁻⁷ MPa or even less, have been reported by Niimi et al.¹² These materials reveal a nonlinear dependence of resistivity from temperature and a considerable PTCR jump upon a post-sintering annealing treatment in air at moderate temperatures around 1000 K. The observed PTCR effect has been ascribed to the amphoteric chemical nature of the rare-earth elements added as dopant. Depending on the ionic radius of the respective rare-earth ion incorporated into the perovskite lattice of barium titanate, preferentially either the Ba- or the Ti-site can be occupied in general. In the amphoteric case, however, trivalent dopants such as the ions Nd³⁺ or Sm³⁺ may enter both crystallographic positions acting as acceptor and donor simultaneously. Yet, even La-doped hypostoichiometric BaTiO₃ ceramics show a pronounced PTCR effect after reductive sintering and a respective reoxidation treatment, although La³⁺ represents a pure donor ion which only substitutes the Ba²⁺-ion in the perovskite lattice.¹³

The questions, why in all cases stoichiometric compositions without any BaO-excess doped with rare-earth elements do not show any PTCR-type behaviour and why the resistivity jump is enhanced upon increasing the amount of BaO added have not been answered yet, although it is known that at elevated temperatures BaTiO₃ exhibits an appreciable solubility of excess BaO.¹⁴⁻¹⁵ The conductivities of BaTiO₃ ceramics containing excessive BaO have been studied in this context by Yeo et al.¹⁶ in detail depending on temperature and partial pressure of oxygen. Their conclusions regarding the influence of BaO-excess on the lattice disorder in BaTiO₃, however, were not related to any further doping for practical applications. For this reason, the present contribution addresses the role of excessive BaO on the defect chemistry of donor-doped BaTiO₃ in order to clarify the fundamental mechanisms that are responsible for the generation of the PTCR-effect in reduction resistant thermistor ceramics of this system. The defect chemical relations were examined by means of DC-conductivity measurements depending on the oxygen partial pressure in an intermediate temperature range between 973 K and 1273 K, which represents the typical thermal regime for the post-sintering reoxidation treatment, where the PTCR effect develops.

2. Experimental

La-doped BaTiO₃ powders were prepared by conventional solid-state reaction, the so-called mixed oxide route. Intimate mixtures of BaCO₃, TiO₂ (rutile) and La₂O₃ powders with additions of colloidal silica were calcined in air at 1323 K for two hours. BaCO₃ (purity > 99 %) and TiO₂ (purity > 99.9 %) were purchased from Sigma-Aldrich, USA, and La₂O₃ (purity 99.999 %) from Alfa Aesar, United Kingdom.

The nominal compositions were prepared according to the formula (Ba_{0.998}La_{0.002})_mTiO₃. The degree of non-stoichiometry expressed by the (Ba+La)/Ti ratio *m* was varied systematically between 1.00 and 1.05. 0.7 wt.-% of colloidal silica was added to each formulation respectively as sintering flux in order to enhance densification during sintering. As binder 3 wt.-% of poly-vinyl acetate (PVAc, Zschimmer & Schwarz, Mohsdorf GmbH & Co KG, Germany) were added to the calcined powders which were then pelletized with a steel die into cylindrical green bodies by uniaxial cold compaction applying a pressure of 100 MPa. These green compacts were then decarbonized at 873 K in air for 10 hours and finally sintered for two hours at 1573 K in a moist gas mixture of Ar and H₂, which resulted at this temperature in a partial pressure of oxygen of approximately 10⁻⁹ MPa. For reoxidation after sintering under these reducing conditions the consolidated ceramic pellets were annealed at 973 K in ambient air. In an analogous way Nb-doped ceramic reference samples with BaO-excess have been prepared, following exactly the same route. They were needed in order to clarify, if the site occupancy of the donor affects the defect chemistry of reduction resistant BaTiO₃ thermistors or not. In contrast to La³⁺, which exclusively occupies the Ba-site of the perovskite lattice, Nb⁵⁺ is completely incorporated on the Ti-site.

Phase purity was inspected by X-ray diffraction (XRD) using a goniometer in Bragg-Brentano – configuration with a Cu-K_α X-ray source (X'pert system, Philips, The Netherlands). The measuring conditions were typically: (i) angular range of Bragg reflections: 20° to 100° and (ii) scanning speed: 0.25°min⁻¹. The lattice parameters were determined through Rietveld-refinements obtained from these measurements. Microstructural analysis of the reoxidized ceramics included observation by scanning and high-resolution transmission electron microscopy (SEM: S-4100, Hitachi, Japan; HR-TEM: JEM-3200, Jeol, Japan). The investigation of the electrical characteristics focussed essentially on measurements of the DC-conductivity in dependence on temperature and partial pressure of oxygen. For this purpose the ceramic samples were connected to a current source (6220, Keithley, USA) and a voltmeter (PM2534, Philips, The Netherlands) according to the four point geometry. During the measurement, the samples were kept in the centre of a gas-tight quartz tube that was placed into a tube furnace. Inside the quartz tube the samples were contacted tightly using Pt-wires. The temperature inside the furnace was monitored with a thermocouple and the partial pressure of oxygen $p(O_2)$ was controlled in the regime between 10⁻²¹ MPa and 10⁻¹ MPa with an oxygen electrolytic pump (SEMG5, Zirox GmbH, Germany) connected at the gas inlet side of the quartz tube in order to adjust the $p(O_2)$ of inflowing dry or humidified gas mixtures of H₂ and Ar. Simultaneously the $p(O_2)$ of the exhaust gas at the outlet of the tubular quartz sample recipient was recorded with an oxygen sensor (Zirox GmbH, Germany).

Additionally in-situ impedance spectroscopic measurements have been carried out in order to determine the frequency dependent AC-conductivity as a function of the partial pressure of oxygen. In this case an Impedance - Gain phase analyser (Schlumberger Instruments, SI 1260, United Kingdom) with dielectric interface (Solatron Analytical, Model 1296, United Kingdom) was connected according to the 2 point geometry to the sample inside the quartz recipient.

3. Materials characteristics

It is well accepted that an electrically insulating grain boundary layer predominately determines the PTCR effect in donor-doped BaTiO₃ ceramics with semiconducting grain cores.^{6, 7} The present contribution focuses on the influence of BaO-excess on the PTCR-characteristics and more specifically on the related point defect chemical relations of such materials. Since the solubility of BaO in BaTiO₃ is believed to be rather small (less than 100 ppm)¹³ the effect of overstoichiometry on the microstructure, phase purity and on the crystallography of the perovskite lattice of the corresponding BaO-rich ceramics have been studied carefully first before investigating the electrical characteristics, related to the PTCR-effect.

3.1. Microstructural and crystallographic analysis

SEM, HR-TEM and XRD in conjunction with Rietveld analyses have been used in order to clarify the influence of excessive BaO on the microstructural and crystallographic characteristics of the reduction resistant thermistor ceramics of this study. Fig. 1 exemplarily shows some selected fracture surfaces of La-doped (0.2 at.-%) ceramics depending on the (Ba+La)/Ti ratio m , as they have been observed by SEM. A statistical quantification of the influence of m on the average grain size determined using a computer-assisted method is also presented in Fig. 1.

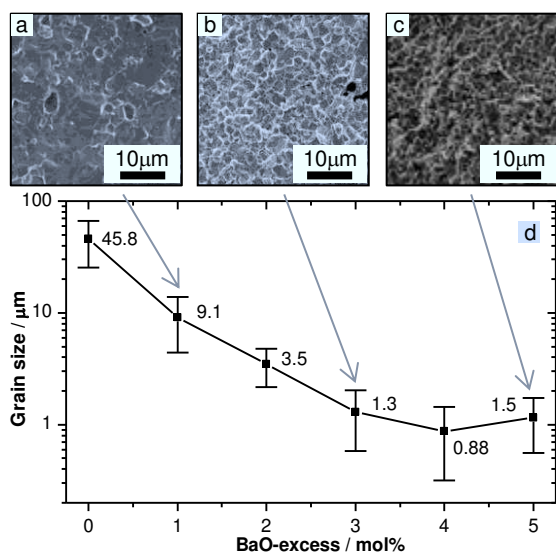


Fig. 1 Fracture surfaces and derived average grain sizes of $(\text{Ba}_{m-0.002}\text{La}_{0.002})\text{TiO}_3$ ceramics with various BaO-excess sintered at 1573 K and $p(\text{O}_2) = 10^{-9}$ MPa: (a) $m = 1.01$, (b) $m = 1.03$ and (c) $m = 1.05$. The representation in (d) shows the influence of excessive BaO on the average grain size. The numbers inside the graph represent average numerical values in μm and the bars through the data points the experimental error.

Under identical sintering conditions and at the same level of donor doping, excessive BaO effectively reduces the average grain size in BaTiO₃-based PTCR ceramics down to approximately 1 μm for compositions with 4 mol.-% or more of additional BaO. This refinement in microstructure is related with a corresponding increase of the volume fraction of resistive grain boundaries in the ceramics. Accordingly, from an electrical point of view, a marked decrease of DC-resistivity is anticipated with increasing BaO-content.

Fig. 2 represents the effect of extra BaO on the phase purity of overstoichiometric La-doped BaTiO₃ ceramics sintered under reducing conditions. Surprisingly no additional reflection peaks, other than the ones belonging to the tetragonal polymorph of phase pure barium titanate could be identified in the XRD patterns shown here up to a (Ba+La)/Ti ratio m as high as 1.03. Because of the very limited solubility of the BaTiO₃ lattice for additional BaO at low temperatures, this result seemed unexpected at a first glance. For compositions exceeding 3 mol.-% of BaO-addition additional reflection peaks arising from barium orthotitanate could be found.

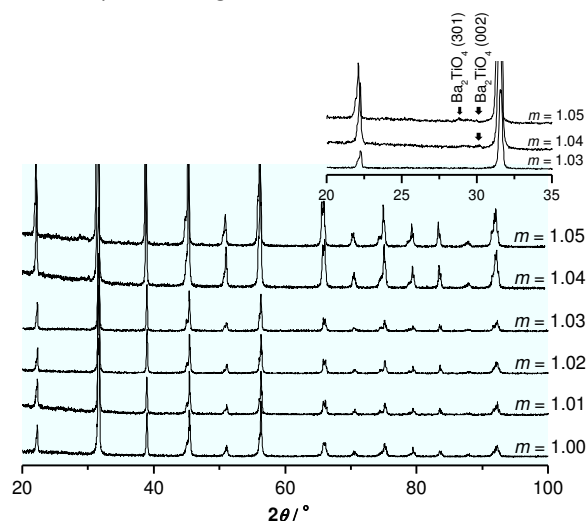


Fig. 2 XRD-patterns recorded for $(\text{Ba}_{m-0.002}\text{La}_{0.002})\text{TiO}_3$ ceramics with various (Ba+La)/Ti ratios m up to $m = 1.05$ sintered at 1573 K and $p(\text{O}_2) = 10^{-9}$ MPa. The inset shows a magnified view on the range of double Bragg-reflection angles between 20° and 35° and gives evidence for the presence of barium orthotitanate Ba_2TiO_4 for compositions with more than 4 mol.-% of BaO addition.

Other impurities expected from the addition of the sintering flux SiO_2 ¹⁷⁻¹⁸ are phases of the type BaTiSiO_5 or $\text{Ba}_2\text{TiSi}_2\text{O}_8$ (fresnoite) originating from the system $\text{BaO-TiO}_2\text{-SiO}_2$. Very few localized inclusions of such secondary phases on the grain boundaries could in fact be identified by HR-TEM in combination with EDX (energy dispersive X-ray spectroscopy).

In summary, the extent of phase impurities and secondary phases through the addition of BaO appears to be less pronounced compared to the strong effect of grain refinement excessive BaO causes.

Therefore, the assumption arose, that in fact the perovskite lattice of BaTiO₃ tolerates larger amounts of soluble BaO even at low temperatures surpassing the limits reported in the literature so far.

However, Rietveld refinements for the crystallographic parameters of the perovskite unit cell of La-doped BaTiO₃ with BaO excess sintered under reducing conditions, obtained from the experimental data shown in fig. 2 revealed that actually both the dimensions of the a-axis (399.33 ± 0.07 pm) and of the c-axis (402.80 ± 0.09 pm) are practically independent of the amount of excessive BaO. The dependence of these lattice parameters on the BaO-content added is represented in fig. 3.

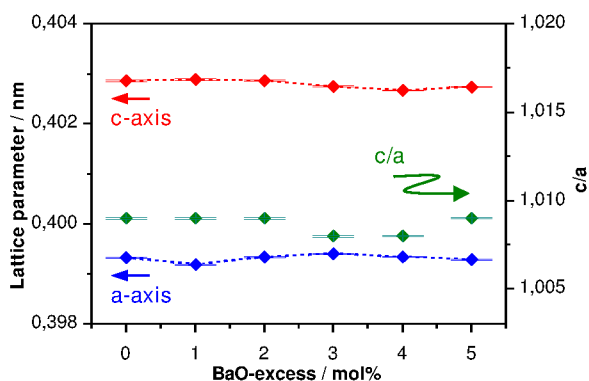


Fig. 3 Dependence of the lattice parameters *a* and *c* as well as of the tetragonality ratio *c/a* of the tetragonal perovskite lattice at room temperature for (Ba_{*m*-0.002}La_{0.002})TiO₃ with various (Ba+La)/Ti ratios *m* up to *m* = 1.05 sintered at 1573 K and *p*(O₂) = 10⁻⁹ MPa. The horizontal lines through the data points reflect the experimental error.

The results in fig. 3 certainly favour the conclusion that the incorporation of BaO into the bulk volume of the perovskite phase is very limited. Still, however, the possibility of locally enhanced BaO-uptake in regions close to the grain boundaries, especially in very fine-grained ceramics had to be taken into consideration. As a result, the formation of extended crystal defects in the grain boundary regions could be anticipated. For this reason, the microstructures were studied in more detail using high-resolution transmission electron microscopy HR-TEM. Fig. 4 shows three HR-TEM images taken from (a) an inclusion of a Si-containing fresnoite impurity, (b) a grain of the ceramic BaTiO₃-matrix and (c) a grain-boundary of two adjacent BaTiO₃-grains respectively.

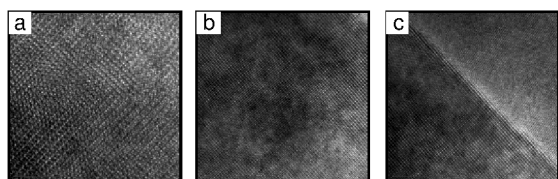


Fig. 4 HR-TEM images of the crystal lattices of (a) a fresnoite inclusion, (b) a grain of the ceramic BaTiO₃-matrix and (c) of a large angle grain-boundary of two neighbouring grains of BaTiO₃. The composition of the thermistor ceramic shown here had the highest (Ba+La)/Ti ratio *m* = 1.05 studied in this report. Even at such a high amount of excessive BaO no evidence for the existence of extended defects in the grain-boundary regions could be found.

No extended defects in the form of layered crystallographic superstructures as they are sometimes reported to exist¹⁹ could be evidenced. The grain boundaries seem to be crystallographically sharp and the atomic arrangement in these internal interfaces resembles to that in the grain interior. Although the presence of extended defects in overstoichiometric BaTiO₃ cannot be excluded completely, it is plausible to assume and conclude that excessive BaO is at least partially incorporated into the perovskite lattice around the

grain boundaries, even if the solubility is low. One argument that supports this hypothesis is the fact that grain growth is strongly inhibited by the addition of BaO. Therefore, it is very probable that enhanced concentrations of BaO prevail in the intragranular regions.

3.2. PTCR-characteristics

For all material compositions investigated in the present study no PTCR-effect could be observed directly after sintering under reducing conditions.

The desired non-linearity of resistivity enhancement only developed during a post-sintering reoxidation annealing treatment, typically carried out in air at a temperature of 973 K. Fig. 5 indicates the corresponding PTCR-characteristics obtained, representing the temperature dependence of resistivity for BaTiO₃-based thermistor ceramics with a BaO-excess ranging from *m* = 1.00 up to *m* = 1.05.

The results shown in fig. 5 clearly demonstrate that the BaO excess represents an essential and indispensable prerequisite for realizing the PTCR effect in reoxidized BaTiO₃ sintered under reducing conditions. The stoichiometric composition with *m* = 1.00 does not show any non-linearity in resistivity but a rather flat temperature characteristics at a nearly constant level of resistivity around 20 Ωcm. A distinct jump in resistivity upon heating only occurs for ceramics with *m* being larger than 1.01. The richer the composition is in BaO the more pronounced is this jump and the higher is the value of cold resistivity, below the Curie temperature *T*_C. The latter effect is thought to be related to the refinement of the microstructure upon BaO addition. Since the grain boundaries are more resistive than the semiconducting cores of the BaTiO₃ grains and because a smaller grain size implies a larger volume fraction of these resistive interfaces, finer grained ceramics become more insulating compared to coarser ones. A very noticeable resistivity jump exceeding over at least two orders of magnitude is observed when *m* becomes larger than 1.02. The largest resistive increase upon heating above *T*_C develops for the case *m* = 1.03, where even three orders of magnitude are achieved.

4. Defect chemical analysis and discussion

4.1. Kröger-Vink representations: Experiment vs. Simulation

Generally¹⁰ three types of possible intrinsic defect chemical reactions are considered in undoped BaTiO₃: (i) electronic disorder based on electron-hole recombination, (ii) the redox equilibrium causing the formation of oxygen vacancies $V_{O}^{\bullet\bullet}$ under the release of O₂ to the atmosphere and (iii) the Schottky reaction resulting in vacancies on all lattice sites of the perovskite crystal structure. Each of these reactions can formally be described by the law of mass action, which relates the concentration of the defects involved in these reactions with the respective thermodynamic parameter.¹⁰ The corresponding equations are represented in the order mentioned above for all three cases, using the formalism by Kröger and Vink:²⁰

$$\text{nil} \rightleftharpoons e + h \quad (1)$$

$$K_e = n \cdot p = N_c \cdot N_v \cdot \exp\left(\frac{-E_g}{k_B \cdot T}\right) \quad (2)$$



$$K_r = \sqrt{p(\text{O}_2)} \cdot n^2 \cdot [\text{V}_\text{O}^{\bullet\bullet}] = N_r \cdot \exp\left(\frac{-E_r}{k_B \cdot T}\right) \quad (4)$$

$$\text{nil} \rightleftharpoons \text{V}_{\text{Ba}}'' + \text{V}_{\text{Ti}}'' + \text{V}_\text{O}^{\bullet\bullet} \quad (5)$$

$$K_s = [\text{V}_{\text{Ba}}''] \cdot [\text{V}_{\text{Ti}}''] \cdot [\text{V}_\text{O}^{\bullet\bullet}] = N_s \cdot \exp\left(\frac{-E_s}{k_B \cdot T}\right) \quad (6)$$

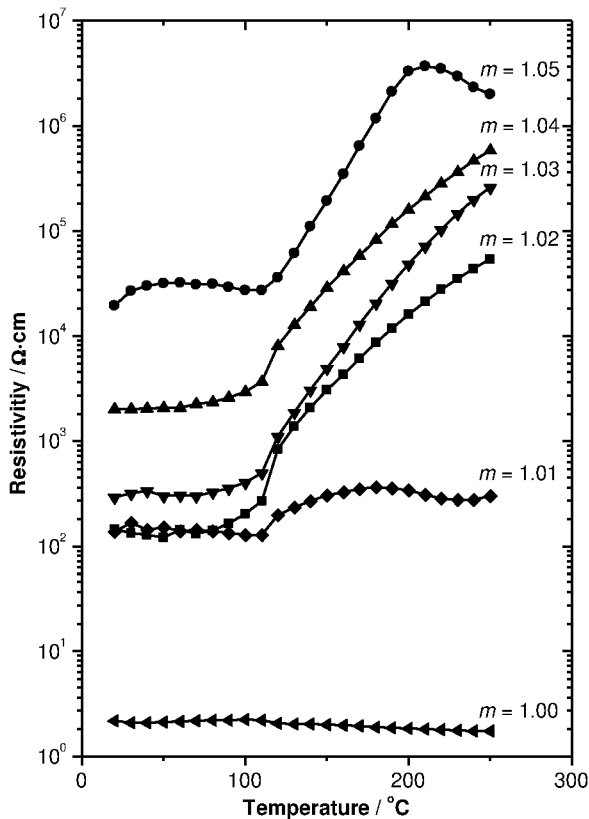


Fig. 5 Temperature dependence of total resistivity for ceramic compositions $(\text{Ba}_{m-0.002}\text{La}_{0.002})\text{TiO}_3$ with various $(\text{Ba}+\text{La})/\text{Ti}$ ratios m ranging between 1.00 and 1.05 sintered at 1573 K and $p(\text{O}_2) = 10^{-9}$ MPa after subsequent reoxidation at 973 K in air for two hours.

Equations (1), (3) and (5) denote the respective defect chemical equilibria and equations (2), (4) and (6) the corresponding laws of mass action. The thermodynamic quantities in the latter relations N_c (effective density of states in the conduction band), N_v (effective density of states in the valence band), N_r and N_s that define pre-exponential constants and the activation energies E_g (band gap energy), E_r and E_s can be derived from data reported elsewhere.¹⁰ It should be pointed out that the exchange kinetics of oxygen (equation 3) is generally only active in perovskite type titanates at temperatures above around 770 K and that the Schottky reaction remains essentially frozen below approximately 1470 K, because of the low diffusivity of cationic vacancies.

Using the before mentioned thermodynamic constants, all concentrations of point defects can be calculated as a function of the absolute temperature T , the partial pressure of oxygen $p(\text{O}_2)$ and – in the case of the present donor-doped thermistor

ceramics – of the concentration of donor ions incorporated into the lattice $[\text{La}_{\text{Ba}}^\bullet]$ using the condition of electrical neutrality:

$$p + 2[\text{V}_\text{O}^{\bullet\bullet}] + [\text{La}_{\text{Ba}}^\bullet] = n + 2[\text{V}_{\text{Ba}}''] + 4[\text{V}_{\text{Ti}}'''] \quad (7)$$

A more comprehensive and detailed description of the calculation procedure used to simulate the concentrations of electrons n , holes p and all other point defects is outlined by one of the authors elsewhere.²¹ Calculated Kröger-Vink diagrams visualize and predict the prevailing defect chemical mechanisms, that can be expected theoretically under the assumption of different possible practical scenarios.

In consequence, experimental and theoretical data can be compared.

Fig. 6 shows exemplarily a Kröger-Vink representation that reveals the dependence of the DC-conductivity from the partial pressure of oxygen at 1273 K obtained for a thermistor composition with a relatively low BaO-excess m of only 1.01, showing a rather modest PTCR-effect. The results compare experimentally determined conductivity values (black symbols) and theoretically expected values obtained from simulation calculations for the two opposite situations, that the Schottky reaction is either active (red curve) or completely frozen in (blue curve).

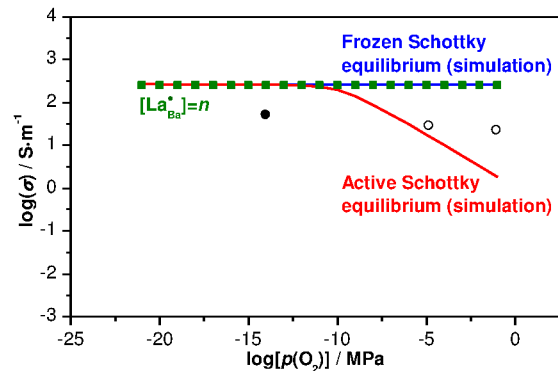


Fig. 6 Dependence of DC-conductivity for $(\text{Ba}_{1.008}\text{La}_{0.002})\text{TiO}_3$ at 1273 K from the partial pressure of oxygen $p(\text{O}_2)$. The black symbols represent experimentally determined values obtained after full equilibration (full symbol) and measured 24 hours after the adjustment of temperature and oxygen partial pressure (open symbols). The blue and red curves correspond to theoretical predictions, calculated from the concentration of free electrons n for the case that the Schottky reaction is assumed to be active (red curve) or frozen (blue curve). The green squared full symbols mark the conductivity expected for the supposed situation that the donor concentration of 0.2 mol-% of La is fully incorporated into the perovskite lattice.

The experimental plateau region in fig. 6, for which the electron concentration is expected to be governed by the amount of donor addition ($n \approx [\text{La}_{\text{Ba}}^\bullet]$) is located at a conductivity level of $10^{+1.7}$ S·m⁻¹ (full black symbol). From this conductivity value and assuming a typical electron mobility value of $\mu_e = 0.50$ cm²·V⁻¹·s⁻¹¹⁰ the concentration of free electrons n can be calculated to be approximately 6.9×10^{18} cm⁻³. This concentration is lower than the theoretically expected one (3.1×10^{19} cm⁻³) which would be obtained if the addition of the La-donor is fully incorporated into the lattice and if all donor ions are completely ionized (green full squared symbols in fig 6.).

Still, however, the experimental values fall within a reasonable range, from what would be expected from the theoretical point of view. Nevertheless, it must be concluded that actually not all donors are compensated by electrons¹¹.

In the oxidizing regime above approximately $p(\text{O}_2) = 10^{-10}$ MPa a reliable measurement of DC-conductivity at intermediate temperatures below 1470 K is problematic due to the slow kinetics of metal vacancies equilibration.

The experimental results (open black symbols) shown for $m = 1.01$ in fig. 6 represent values that have been recorded 24 hours after adjusting temperature and oxygen partial pressure. It is evident that these data do not correspond to the thermodynamic equilibrium, because they are situated between the two opposite extreme cases of a completely frozen Schottky equilibrium (blue curve) and of fully active metal vacancy compensation (red curve). These results show that the Schottky reaction is, even at intermediate temperatures as low as 1273 K, at least partially operative.

The formation of metal vacancies in the oxidizing regime apparently takes place only very slowly and locally restricted, presumably starting from grain boundary regions. It is important to keep this fact in mind when analysing the defect chemical situation of the technical material compositions of the present study.

4.2. Kröger-Vink representations: Effect of the BaO-excess

Fig. 7 represents experimentally determined Kröger-Vink diagrams recorded in the temperature range from 973 K to 1273 K for compositions with 1, 3 and 5 mole percent of BaO-excess ($m = 1.01, 1.03$ and 1.05). The open symbols denote again “non-saturated values” that were measured after keeping the temperature and partial pressure of oxygen at a constant level. The full symbols stand for experiments, for which equilibration was reached.

For the compositions with a relatively large excess of BaO the $p(\text{O}_2)$ dependence of DC-conductivity differs quite strongly from the experimental results obtained for the case of $m = 1.01$ and from the calculated curves previously presented in fig. 6. In both cases $m = 1.03$ and $m = 1.05$ essentially similar characteristics are observed. At strongly reduced partial pressures of oxygen the slope is always negative and at high $p(\text{O}_2)$ -values above $10^{-7} - 10^{-5}$ MPa the slope is flat or even positive in the double logarithmic plot.

Interesting to note in this context is the fact that the shape of the curves obtained for $(\text{Ba}_{1.048}\text{La}_{0.002})\text{TiO}_3$, the composition with the highest excess in BaO, remarkably resemble to typically acceptor doped BaTiO_3 ,^{13,17} although the net composition is actually donor doped. At low partial pressures of oxygen, the slope almost perfectly corresponds to a value of $-1/6$. In the oxidizing regime, however, the slope is very close to the value $+1/4$. Both these respective parts of the conductivity curves meet in a point of minimum conductivity, which is referred to – in the case of acceptor doped BaTiO_3 – to the so-called intrinsic minimum of conductivity, where the concentration values of electrons n and of defect electrons or holes p are exactly identical. Therefore, this transition point marks a change of the conduction mechanism from n- to p-type semiconduction. The

intermediate range of oxygen partial pressures could, however, not be assessed in a reliable manner with the available experimental setup because of the difficulty to control and maintain intermediate values of $p(\text{O}_2)$ properly.¹⁵

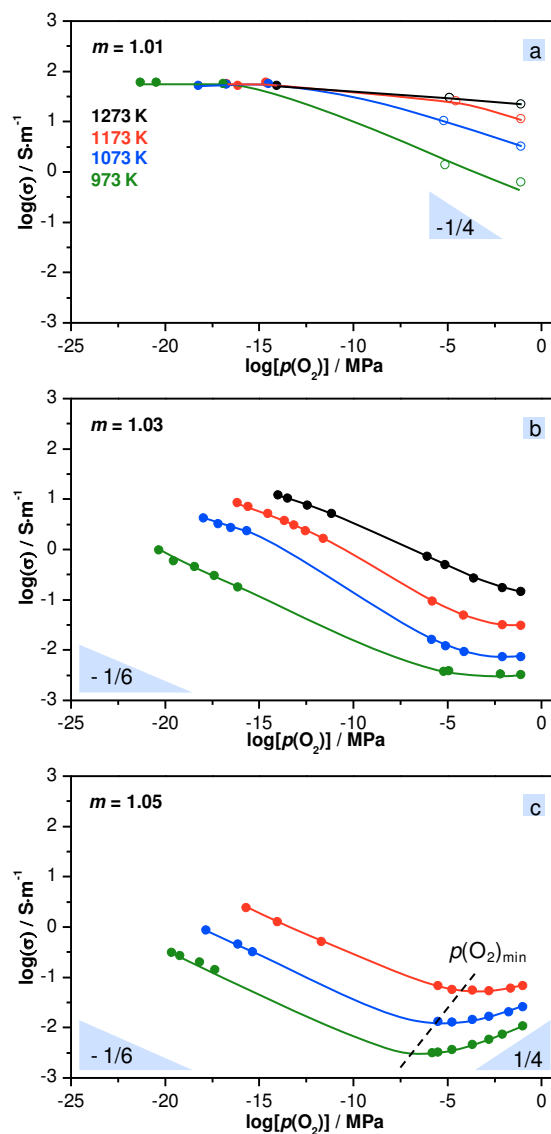


Fig. 7 Experimentally determined Kröger-Vink diagrams showing the $p(\text{O}_2)$ dependence of DC-conductivity for measuring temperatures in the range from 973 K to 1273 K. Three cases are considered here: La-doped BaTiO_3 with (a) 1 mol.-% ($m = 1.01$), (b) 3 mol.-% ($m = 1.03$) and (c) 5 mol.-% ($m = 1.05$) of BaO-excess. Open symbols represent conductivity measurements carried out after keeping the respective temperature and value of $p(\text{O}_2)$ constant for 24 hours and the full symbols denote data recorded after full equilibration of conductivity.

Compared to the theoretically expected values of conductivity and assuming that all donors are fully incorporated and ionized ($\sigma = 10^{+2.55}$ S·m at 1273 K) the observed values for the maximum conductivity in figures 7 (b) and (c) are significantly smaller ($\sigma = 10^{+1.05}$ S·m for $m = 1.03$ at 1273 K and for $p(\text{O}_2) = 10^{-14}$ MPa; $\sigma = 10^{+0.38}$ S·m for $m = 1.05$ at 1173 K and for $p(\text{O}_2) = 10^{-15.7}$ MPa). This difference amounts to one or two orders of magnitude.

Apparently the BaO-rich compositions behave in total electrically more insulating compared to ceramics with low (Ba+La)/Ti ratio m .

In order to clarify this discrepancy impedance spectroscopy carried out in situ under reducing conditions has been performed at 973 K and $p(\text{O}_2) = 10^{-21}$ MPa in the frequency range from 100 mHz up to 1 MHz for a composition with a rather low BaO-content ($m = 1.01$) in comparison to a BaO-rich composition ($m = 1.05$).

The results are displayed in fig. 8. Under identical measurement conditions, the material with higher BaO-excess reveals a considerably higher DC-resistance compared to the relatively BaO-poor composition. In the case of $m = 1.05$ a nearly semicircular shaped, strongly depressed frequency arc was obtained, whereas for $m = 1.01$ no such locus could be observed. Since no semicircle is found in $m = 1.01$ the existence of insulating barrier layers at the electrode-ceramic interface could be excluded. The arc measured for the BaO-rich composition with $m = 1.05$ is presumably arising from the resistive and capacitive contribution of insulating grain boundaries. It can therefore be concluded that the difference of DC-conductivity in BaO-rich compositions results from additional contributions of the more insulating grain boundaries, whereas in BaO-poor materials only the semiconducting bulk appears. The results from Moos et al. support this interpretation.²² Moos et al. presumed from high temperature conductivity measurements on $\text{Sr}_{1-x}\text{La}_x\text{TiO}_3$ single crystals and ceramics an involvement of grain boundaries in the case of polycrystalline specimens.

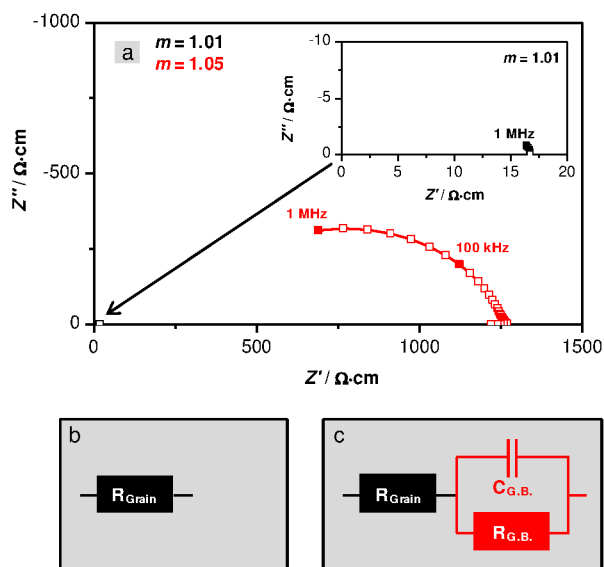


Fig. 8 (a) Impedance spectroscopic analysis performed in situ under reducing conditions at 973 K and an oxygen partial pressure of $p(\text{O}_2) = 10^{-21}$ MPa. The La-concentration is 0.2 at.-%. Black symbols correspond to a BaO-excess of 1 mol.-% (an enlarged view of the spectrum is shown in the inset) and the red symbols to a BaO-excess of 5 mol.-%. The frequency range was 100 mHz to 1 MHz. The corresponding equivalent circuits used to explain these spectra are illustrated in (b) for the case of $m = 1.01$ and in (c) for the case of $m = 1.05$. The indices "Grain" and "G.B." in the subscript of the resistance R and capacitance C denote the contribution of the bulk and of the grain boundaries respectively.

As stated before the slopes of the modified Kröger-Vink diagrams from fig. 7(b) and fig. 7(c) correspond to a value close to $-1/6$ in the regime of low $p(\text{O}_2)$. A theoretical value of $-1/6$ is expected when the electron concentration is governed by doubly charged oxygen vacancies $n \approx 2[V_{\text{O}}^{**}]$ according to the law of mass action represented by equation (4). Fig. 9(b) shows an Arrhenius representation of the electrical conductivity of $(\text{Ba}_{1.048}\text{La}_{0.002})\text{TiO}_3$ measured at different temperatures and an oxygen partial pressure $p(\text{O}_2)$ of 10^{-16} MPa in comparison to data reported by Chan et al.²³ for nominally non-doped BaTiO_3 . It should be recalled in this context that even intentionally non-doped BaTiO_3 always contains minor but not negligible concentrations of acceptors because the Ti-compounds used as raw materials for the synthesis are never absolutely pure. In the case of reducing conditions (fig. 9(b)) the activation energy of conduction amounts to approximately 1.8 eV, a value that corresponds to the one reported by Chan et al. (2.0 eV). Both observations made in the regime of low partial pressures of oxygen $p(\text{O}_2)$, the slope of $-1/6$ in fig. 7 and the value of the activation for electrical conduction allow the final conclusion that intrinsic reduction of BaTiO_3 is taking place in this region.

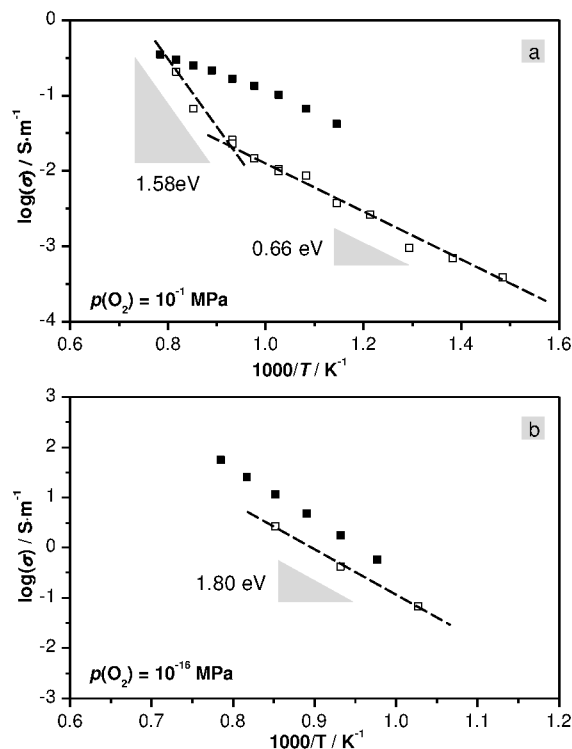


Fig. 9 Temperature dependence of conductivity σ for $(\text{Ba}_{1.048}\text{La}_{0.002})\text{TiO}_3$ (open symbols) compared to data reported by Chan et al.²³ for nominally pure BaTiO_3 (closed symbols) determined in (a) pure oxygen ($p(\text{O}_2) = 0.1$ MPa) and (b) at $p(\text{O}_2) = 10^{-16}$ MPa.

In the regime of higher partial pressures of oxygen $p(\text{O}_2)$ ranging from approximately 10^{-6} MPa to 0.1 MPa the conductivity behaviour of BaO-rich PTCR compositions is quite striking. For $m = 1.03$ the electric conductivity still declines with increasing $p(\text{O}_2)$ but this dependence becomes weaker the lower the temperature is. In the case of $m = 1.05$, however, conductivity is enhanced with increasing $p(\text{O}_2)$.

The respective positive slope in the modified Kröger-Vink diagram indicates p-type semiconductivity. On the first sight, it appears to be surprising that in spite of a net donor doped material p-type behaviour is observed. Apparently, the dominating insulating effect of the grain boundaries prevails here. This characteristic is also supported by results obtained from measurements of the thermoelectric power, which are shown in fig. 10.

In the case of low BaO-excess ($m = 1.01$, fig. 10(a)) perfect accordance with n-type semiconduction was found (Seebeck coefficient $S = -600.4 \mu\text{V/K}$). BaO-rich compositions, however, reveal a more complex characteristics ($m = 1.05$, fig. 10(b)), most likely due to the electrical non-homogeneity of the material caused by the overlapping contributions of n-type grains and p-type grain boundaries. It is known that such mixed conduction may reduce the absolute value of the Seebeck coefficient.²⁴ The value of the Seebeck coefficient obtained for $m = 1.01$ corresponds to the range reported by other authors^{25,26}, confirming that the experimental determination was conducted in a reliable manner. Yoo et al.²⁷ also report on partial p-type semiconduction in donor-doped BaTiO₃ ceramics by measuring the thermoelectric power. These authors found in particular for B-site deficient Ba_{0.99}La_{0.01}Ti_{0.9975}O₃ that the transference number of electron holes may reach a value of 0.15 and that total electric conduction is therefore determined by 15 % through a p-type mechanism. In this work, partial p-type conduction is related to the formation of Ti-vacancies. Consequently, it can be concluded that p-type conduction is consistent even with globally donor-doped BaTiO₃.

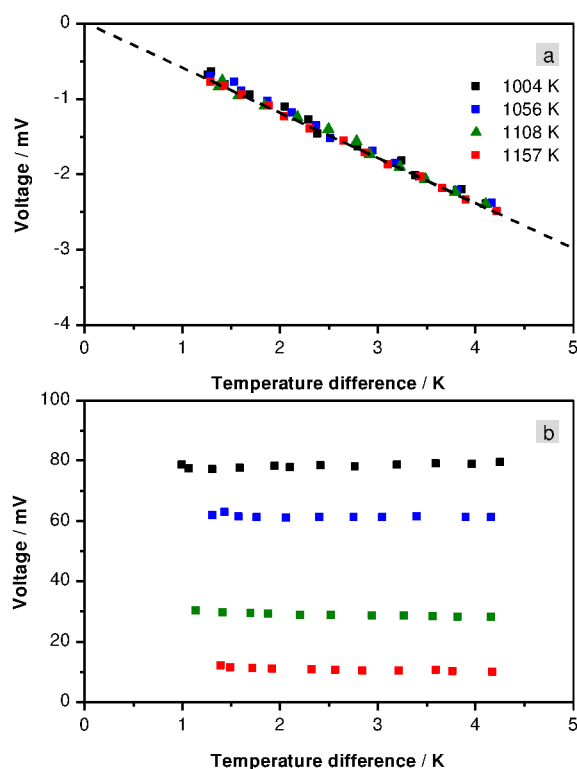


Fig. 10 Dependence of the thermoelectric power from temperature difference for (a) Ba_{1.008}La_{0.002}TiO₃ and (b) Ba_{1.048}La_{0.002}TiO₃ measured at various temperatures in air.

Fig. 9 (a) shows an Arrhenius representation of the conductivity in the p-type regime for the composition Ba_{1.048}La_{0.002}TiO₃ determined at a partial pressure of oxygen of $p(\text{O}_2) = 0.1 \text{ MPa}$ (pure oxygen). These experimental results are again compared with data reported on nominally undoped BaTiO₃.²³ According to these results, the activation energy for electric conduction in BaO-rich PTCR compositions apparently show two different temperature regimes.

At elevated temperatures above 1073 K the activation energy amounts to $1.58 \pm 0.38 \text{ eV}$ and at lower temperatures below 1073 K a smaller value of $0.66 \pm 0.02 \text{ eV}$ is found, which is close to that reported by Chan et al. (0.56 eV).²³ The activation energy for the lower temperature regime was attributed by Chan et al. to the oxidation of BaTiO₃ according to equation 8.



Therefore, the activation energy determined here represents another evidence for p-type conduction, namely indicating the formation of electron holes. A deviating value of the activation energy at high temperatures has also been described by Itoh et al.²⁸ and Shirasaki et al.²⁹⁻³¹ According to their experimental results the activation energy drastically changed from 0.62 – 0.67 eV to 2.32 – 2.88 eV above 1223 K and they attributed this transition to the dissociation of complex defect associates of the type $[\text{V}_\text{O}^{\bullet\bullet} - \text{V}_\text{M}^{\prime\prime}]$ or the additional release of oxygen from the lattice. In both cases, p-type conduction is enhanced due to the increase of the concentration of free oxygen vacancies. Since one oxygen vacancy is correlated with two electron holes the activation energy per charge carrier would be half of the measured value. Possibly the increase of the oxygen vacancy concentration is responsible for the higher conductivity above 1073 K.

In order to clarify the question, how the defect chemistry in the p-type regime affects the PTCR characteristics, the impedance spectra of ceramics that were annealed ex-situ at 973 K for two hours in atmospheres with different partial pressures of oxygen $p(\text{O}_2)$ in the range from 10^{-20} MPa to $10^{-2.5} \text{ MPa}$ after sintering were investigated.

The magnitude of the increase in resistivity ρ above the Curie temperature T_C can be quantified by the PTCR parameter η , which is defined by:

$$\eta = \log \left(\frac{\rho(250 \text{ }^\circ\text{C})}{\rho(20 \text{ }^\circ\text{C})} \right) \quad (9)$$

The resistivity values $\rho(250 \text{ }^\circ\text{C})$ and $\rho(20 \text{ }^\circ\text{C})$ in equation (9) represent the values measured at 523 K (250 °C) and 293 K (20 °C) respectively. The dependence of DC conductivity σ and of the parameter η from the partial pressure of oxygen $p(\text{O}_2)$ applied during post sintering annealing for the composition Ba_{1.048}La_{0.002}TiO₃ is displayed in fig. 11(a). The corresponding temperature characteristics revealing the influence of $p(\text{O}_2)$ on the PTCR effect are represented in fig. 11(b). The results shown clearly prove that the PTCR jump is directly correlated to the conductivity type specified in the modified Kröger-Vink diagram of fig. 11(a), where a drastic increase of η appears when BaO-rich and La-doped BaTiO₃ is annealed at oxygen partial pressures $p(\text{O}_2)$ above $10^{-6.2} \text{ MPa}$.

This significant enhancement is apparently related to the emergence of p-type conductivity at relatively high values of $p(\text{O}_2)$ and connected to the oxidation of the grain boundaries.

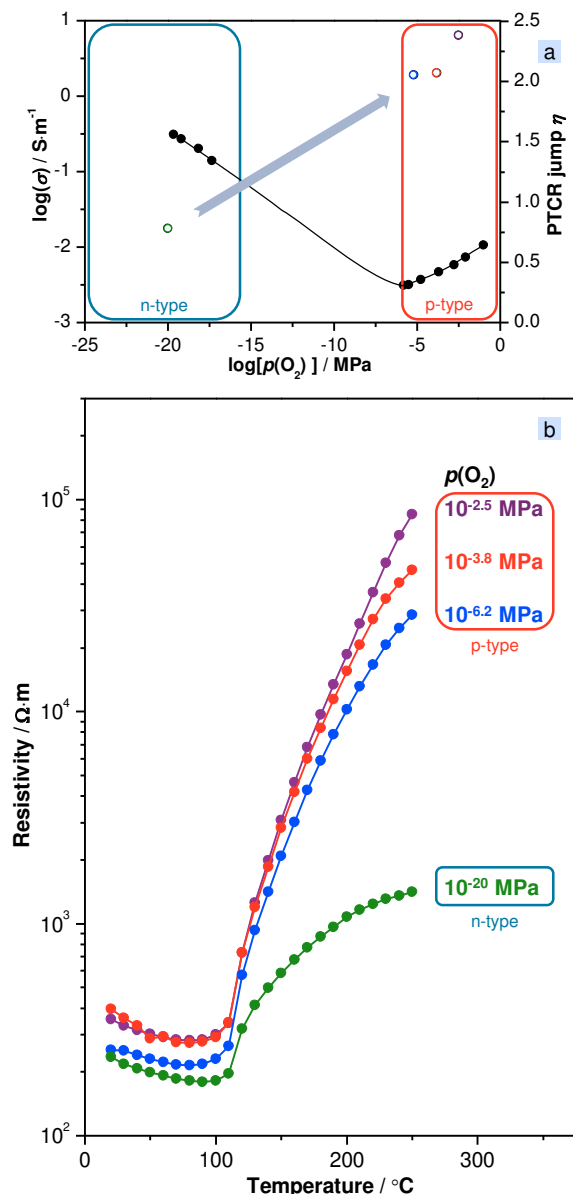


Fig. 11 (a) Dependence of the DC conductivity σ (full, black symbols) and of the PTCR parameter η (open, colored symbols) from the partial pressure of oxygen $p(\text{O}_2)$ at 700 °C for the composition $\text{Ba}_{1.048}\text{La}_{0.002}\text{TiO}_3$. (b) Temperature characteristics of resistivity depending on the partial pressure of oxygen $p(\text{O}_2)$ applied during the post sintering reoxidation treatment.

4.3. The case of Nb-doped BaTiO_3 with BaO-excess

Before concluding the defect chemistry of BaO-excess PTCR compositions based on BaTiO_3 , a possible scenario had to be excluded.

The high amount of BaO added could result in the expulsion of La-donor ions from the A-site of the perovskite crystal structure causing a reduction of the effective donor concentration in the grain interior. Since the donor content of the PTCR ceramics studied in this study is rather low, a direct analytical detection by electron spectroscopic methods, such as

EDX (Energy-dispersive X-ray spectroscopy), is problematic, unless local segregation or enrichment occurs. In order to exclude this hypothetical assumption Nb-doped BaTiO_3 ceramics have been prepared and their electric characteristics were investigated.

The ionic radius of Nb^{5+} -cations (64 pm for six-fold coordination) is very similar to that of Ti^{4+} -cations (60.5 pm for six-fold coordination).³² Due to this reason it is believed that the donor Nb^{5+} preferentially occupies the B-site of the perovskite lattice. Since the chemical compositions studied in this context are rich in BaO, it is highly probable that Nb^{5+} is completely soluble in BaTiO_3 , unless Nb_2O_5 and BaO form secondary phases. Fig. 12 shows the case of Nb-doped (0.2 mol.-%) barium titanate with 5 mol.-% of BaO-excess. The results clearly demonstrate that the PTCR effect in BaO-rich BaTiO_3 does not depend on the kind of donor used. Even if a donor that occupies the B-site is incorporated a strong increase of resistivity at the Curie temperature T_C is obtained, fig. 12 (a). Decisive is the crucial BaO-excess not the type of the donor ion. The modified Kröger-Vink diagram for Nb-doped BaTiO_3 in fig. 12(b) again shows p-type conductivity in the regime of high partial pressures of oxygen. Chan and Smyth³³ reported previously that only a small portion of Nb and as low as 0.02 mol.-% is sufficient to achieve n-type conductivity over the whole $p(\text{O}_2)$ regime considered in the present study.

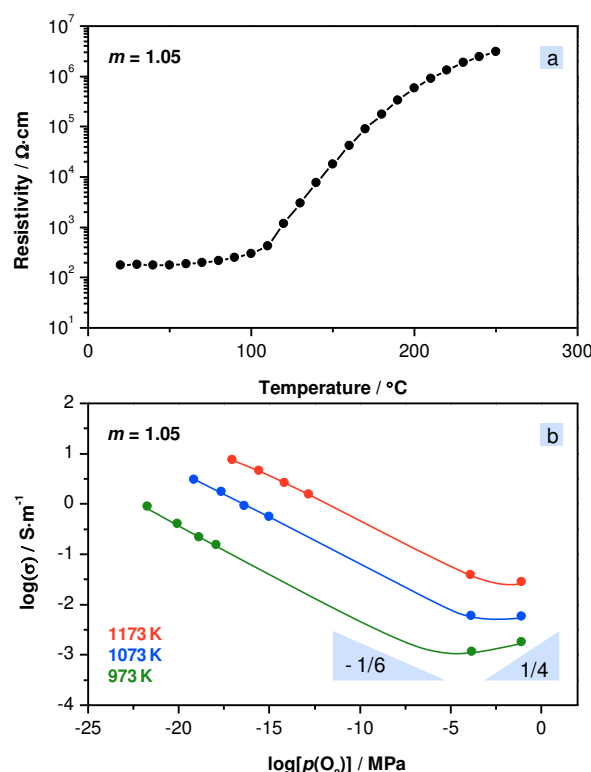


Fig. 12 (a) Temperature characteristics of resistivity and (b) DC conductivity σ in dependence of partial pressure of oxygen $p(\text{O}_2)$ in the intermediate temperature range from 973 K to 1173 K. The materials composition considered here is $\text{Ba}_{1.05}(\text{Ti}_{0.998}\text{Nb}_{0.002})\text{O}_3$ and the electrical properties were determined ex-situ after annealing at 700 °C for two hours in air.

The barium titanate composition described in figure 12 contains a concentration of Nb donors ten times larger than that reported by Chan and Smyth³³, and still reveals the strong p-type (acceptor type) contribution realized by the addition of BaO.

4.4. The case of undoped BaTiO₃ with BaO-excess

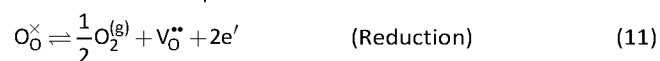
According to the results presented in sections 4.2. and 4.3. only the excess of BaO regarding the materials composition is decisive for the realization of the PTCR-characteristics of reduction resistant thermistor ceramics based on barium titanate. For this reason, the question arose, whether excessive BaO also provokes intrinsically a promotion of p-type conduction in the system BaTiO₃ even if no intentional doping is present. In other words, do additions of BaO to stoichiometric, pure and deliberately undoped barium titanate effectively enhance the concentration of acceptors in the material? In order to answer this question the effect of excessive BaO on the defect chemistry of undoped BaTiO₃ ceramics was investigated.

For this purpose, the positions of the intrinsic minima of conductivity in the Kröger-Vink diagrams were inspected closely.

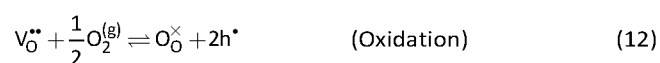
At the intrinsic minimum of conductivity, which corresponds to the partial pressure of oxygen $p(\text{O}_2)_{\text{min}}$ associated with the lowest value of conductivity in the Kröger-Vink representation, the contributions of electrons and electron holes to conductivity, σ_n and σ_h respectively, are equal, as expressed in equation 10.

$$\sigma_n = e \cdot n \cdot \mu_n = e \cdot h \cdot \mu_h = \sigma_h \quad (10)$$

In equation 10 e denotes the elementary charge, n and h the concentration of electrons and electron holes and μ_n as well as μ_h finally the mobility of electrons and electron holes. According to D. M. Smyth³⁴ the intrinsic minimum of conductivity represents the “electronic” stoichiometry point of an oxide material such as barium titanate. When the mobilities of both, electrons and electron holes are equivalent, the intrinsic minimum of conductivity also corresponds to chemical stoichiometry because of the absence of oxygen deficiency or excess. The concentration of electrons n and electron holes h are derived from the law of mass action. The corresponding defect chemical equilibria are:



and



According to the expressions in equation 11 and equation 12 and applying the corresponding equations that represent the respective law of mass action the value of $p(\text{O}_2)_{\text{min}}$ can be represented by

$$p(\text{O}_2)_{\text{min}} = \left(\frac{\mu_n}{\mu_h} \right) \cdot \left(\frac{K_{\text{red}}^0}{K_{\text{ox}}^0} \right) \cdot \exp \left(\frac{\Delta H_{\text{ox}} - \Delta H_{\text{red}}}{k_B \cdot T} \right) \cdot \frac{1}{[\text{V}_\text{O}^{\bullet\bullet}]} \quad (13)$$

K_{red} and K_{ox} are the equilibrium constants for reduction and for oxidation and ΔH_{red} and ΔH_{ox} the corresponding enthalpies for reduction and oxidation respectively.

Assuming that the concentration of oxygen vacancies $[\text{V}_\text{O}^{\bullet\bullet}]$ is governed by acceptor states A' in the region of the conductivity minimum, the next approximation holds:

$$2[\text{V}_\text{O}^{\bullet\bullet}] \approx [A'] \quad (14)$$

Similar expressions to equation 14 can be set up for higher charged acceptors. The relation in equation 14 implies together with equation 13 that the connection between acceptor concentration $[A']$ and $p(\text{O}_2)_{\text{min}}$ can be typified by

$$\left(\frac{\partial \ln p(\text{O}_2)_{\text{min}}}{\partial \ln [A']} \right)_{T=\text{const.}} = -2 \quad (15)$$

This derivative expresses that an increase in the acceptor concentration $[A']$ always brings about a shift of $p(\text{O}_2)_{\text{min}}$ to lower values: quantitatively, a difference of one order of magnitude for $[A']$ results in a shift of $p(\text{O}_2)_{\text{min}}$ by two orders of magnitude.³⁵

Comparing the position of $p(\text{O}_2)_{\text{min}}$ for different BaO additions to pure undoped BaTiO₃ in fig. 13 indeed reveals a shift to lower values of oxygen partial pressure with increasing BaO content. This suggests that BaO-excess in the materials investigated in this study acts as an effective acceptor. The results shown in fig. 13 were obtained by examining the cases of stoichiometric and off-stoichiometric nominally undoped BaTiO₃. Lee et al. reported that the incorporation of excessive BaO into the perovskite lattice of barium titanate requires relatively long heat treatments, because the migration of titanium vacancies involved in this process necessitates a quite large activation energy.³⁶

Therefore three materials conditions were considered to examine the acceptor-effect caused by BaO excess: (i) undoped stoichiometric BaTiO₃ ($m = 1.00$), (ii) undoped over-stoichiometric BaTiO₃ ($m = 1.05$) and (iii) undoped over-stoichiometric BaTiO₃ soaked at 1300 °C for 30 hours after sintering. The samples representing the first two cases (i) and (ii) were only sintered for two hours at 1350 °C. Fig. 13 shows the respective modified Kröger-Vink diagrams. The position of the intrinsic conduction minimum was estimated by extrapolation from the corresponding n-type and p-type branches of the conductivity curves. A comparison of the three different materials conditions is shown in fig. 13(d). It is evident that for all measuring temperatures considered here the position of the intrinsic minimum of conductivity is shifted to lower values of oxygen partial pressure $p(\text{O}_2)$ confirming that incorporation of excessive BaO indeed effectively produces additional acceptor states.

4.5. Final discussion and proposed defect chemical model

In principle – and theoretically – two different possibilities could be envisaged as defect chemical mechanisms to explain the PTCR effect in reduction resistant BaTiO₃-based thermistor ceramics with BaO-excess. The first one is the classical model proposed by Daniels and Wernicke⁹ suggesting the formation of metal vacancies at the grain boundaries.

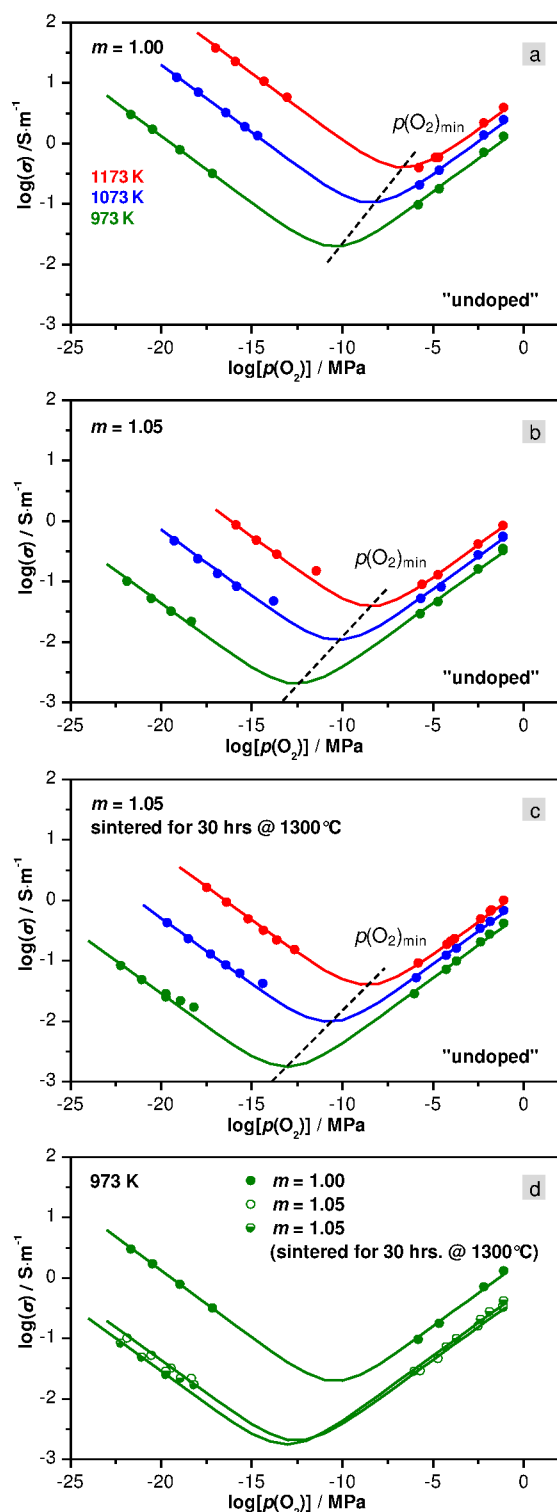
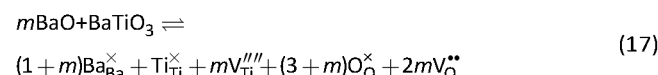


Fig. 13 Modified Kröger-Vink diagrams for (a) stoichiometric ($m = 1$) and (b) hyper-stoichiometric ($m = 1.05$) nominally undoped Ba_mTiO_{3+m} sintered at $1350\text{ }^\circ\text{C}$ for two hours. The case of hyper-stoichiometric $Ba_{1.05}TiO_{3.05}$ that was additionally soaked for 30 hours at $1300\text{ }^\circ\text{C}$ after sintering is shown in (c) and (d) represents a comparison of the conductivity in dependence of oxygen partial pressure $p(O_2)$ of all three materials at 973 K .

The second one relies on the generation of both metal and oxygen vacancies upon the uptake of additional BaO through the perovskite lattice of barium titanate. Both these scenarios can be represented by the following two defect chemical equilibria:



and



The first case can immediately be excluded for the following reasons. Daniels and Wernicke claimed that negatively charged metal vacancies are formed only at the grain boundaries during the cooling process after sintering to compensate the positive charges created by donor doping. In the grain interior, these positive charges arising from donors are balanced by electrons. Their defect chemical model thus described the insulating effect of grain boundaries through the local formation of electrical negative charges at the grain-grain interfaces repelling free electrons in the conduction band of the grain cores.

The responsible reaction for the creation of the negatively charged metal vacancies at the grain boundaries, however, necessitates elevated temperatures above approximately 1300 K and high oxygen partial pressures. Otherwise, electron compensation is more favourable. But high temperatures and large partial pressures of oxygen are contradictory to the processing conditions applied for the realization of reduction resistant BaO-rich compositions of BaTiO₃-based PTCR ceramics. Their distinct and eminent resistivity increase above the Curie temperature T_C evolves after sintering under reducing conditions and after a subsequent annealing treatment at moderate temperatures typically around $700\text{ }^\circ\text{C}$ that are far below the temperature at which the Schottky reaction (equation 6) is active. Thus simple metal vacancy compensation represented by equation 16 does not seem feasible for the materials considered in the present study.

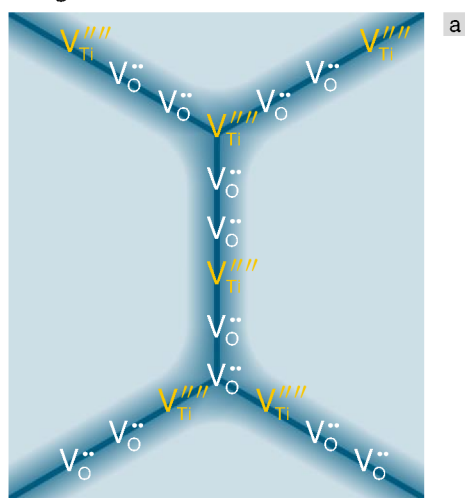
The second scenario presented in equation 16 has to be discussed in a controversial manner. It has been accepted for a long time that the concentration of excessive BaO that can be incorporated into the lattice of BaTiO₃ is relatively small. Hu and Smith³⁷ reported on the basis of defect chemical investigations founded on high-temperature conductivity measurements that the solubility limit of BaO in barium titanate is not larger than 100 ppm. Only rather recently the idea that even more BaO is soluble is supported by several studies. Lee and Randall^{14, 15} reported that at least at elevated temperatures above approximately 1550 K up to 1 mol.-% of BaO could be incorporated into the lattice of BaTiO₃. This temperature regime corresponds to a range in which sintering is typically carried out. Their conclusions were based on differential thermal analysis. Ihlefeld et al.³⁸ even found a total BaO-incorporation into BaTiO₃ thin films up to 5 mol.-%.

Based on this background it is therefore realistic to assume that upon sintering sufficiently large amounts of BaO are soluble in BaTiO₃, at least or in particular in the grain boundary regions.

As expressed in equation 16 extra BaO in the lattice is accompanied by the formation of both titanium and oxygen vacancies. The oxygen vacancies, however, may be easily filled with atmospheric oxygen even at moderate temperatures during a post-sintering annealing treatment.

The titanium vacancies, however, are considered to be frozen in within this temperature range due to their high migration enthalpy.³⁹ Refilled oxygen vacancies act as a source of electron holes as described by equation 12.

According to this reaction p-type conductivity can be expected by the incorporation of excessive BaO into barium titanate and strong experimental evidence for the local existence of p-type semiconduction at grain-boundaries has been communicated in the present study, refer to fig. 7, fig. 12 and fig. 13.



Reoxidation

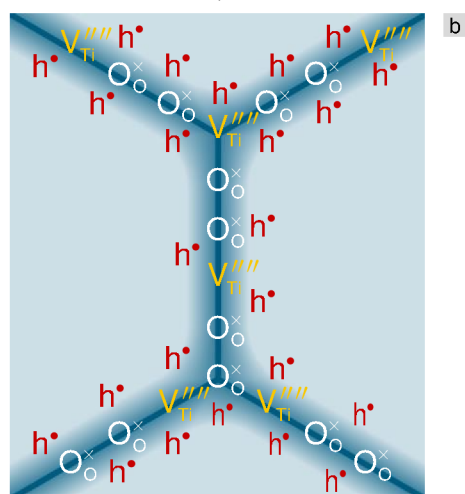
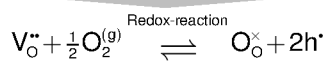


Fig. 14 Schematic representation of the defect chemistry in hyperstoichiometric donor doped barium titanate applied for reduction resistant multilayer thermistors: model of the local defect chemistry at grain-boundaries (a) after sintering or annealing under reducing conditions and (b) after reoxidation.

A concluding schematic and idealized outline that illustrates the defect chemical and electrical character of the grain boundaries in reduction resistant BaTiO₃ thermistor ceramics with BaO-excess after annealing in (a) the n-type and (b) in the p-type regime of partial pressure of oxygen is shown in fig. 14. Due to the relatively short dwelling time during sintering BaO uptake by the perovskite lattice of barium titanate is considered to take place mostly at the grain boundaries resulting in the local formation of both titanium vacancies and oxygen vacancies.

During annealing under oxidizing conditions at sufficiently high partial pressures of oxygen $p(O_2)$ the oxygen vacancies created during sintering are – at least partially – filled by oxygen ions originating from dissociated oxygen molecules from the ambient gas atmosphere.

The oxygen ions preferentially diffuse along the grain boundaries, which could be proven by ¹⁸O-tracer diffusion experiments. The respective results will be published in a second, separate study. In consequence and finally titanium vacancies and electron holes dominate the defect chemistry of the grain-boundaries. During operation of the resulting PTCR material at room temperature or at temperatures below the Curie point T_C electron holes are mostly immobile or captured by the acceptor states constituted by the metal vacancies V_{Ti}''' . This results in the formation of electrically insulating layers at the grain boundaries. The model description is very similar to the widely well accepted concept developed and proposed by Waser et al. regarding the improvement of electrical degradation of insulating dielectric ceramics based on BaTiO₃ sintered under reducing conditions.⁴⁰ At very low partial pressures of oxygen $p(O_2)$ donor-type oxygen vacancies $V_O^{\bullet\bullet}$ represent the majority defect chemical species that release large amounts of free electrons. This causes the annihilation of the electrically insulating layer at the grain boundaries and in consequence, the PTCR effect is expected to degrade.

Summary and Conclusions

The present study examines in detail the dependence of DC-conductivity from temperature T and partial pressure $p(O_2)$ for reduction resistant donor doped BaTiO₃ ceramics with BaO excess as they are applied for the manufacturing of multilayer PTCR thermistors in practice. The Kröger-Vink diagrams that illustrate and summarize this dependence are strongly influenced by the concentration of added BaO, which is incorporated into the perovskite lattice of BaTiO₃ and causes the formation of additional acceptor states preferentially in the grain boundary region. This behaviour is most convincingly but not only evidenced by a shift of the intrinsic minimum of conductivity to lower values of oxygen partial pressure, which also occurs without any donor-doping. In fact the type of donor used, whether A-site or B-site occupancy is applied does not matter. Insulating grain boundary layers showing p-type semiconduction are formed while the grain interior remains n-type conducting. The higher insulation resistance of the grain boundaries originates from the formation of both oxygen and metal vacancies after sintering from which only the oxygen

vacancies are refilled after reoxidation. This particular local defect chemical situation is triggered through the likewise locally enrichment of BaO at these interfaces. Especially the existence of different activation energies for electric conduction in the oxidizing regime strongly support the idea that the creation and dissociation of metal and oxygen defect associates plays an important role.

Conflicts of interest

There are no conflicts to declare.

Acknowledgements

The authors would like to express their sincere gratitude to Prof. Dr. G. Roth and Dr. D.F. Hennings for very fruitful and inspiring discussions on the analysis of point defect chemistry. They acknowledge Dipl.-Ing. J. Friedrich and Mr. M. Gerst for their skilful assistance in setting up the experimental equipment employed in this study. Equally, the authors would like to thank Dr. S. Mi and Dr. J. Lei for the microstructural and analytical characterization by HR-TEM. One of the authors (H.K.) appreciates the financial support from Murata Manufacturing Co., Ltd. for the opportunity to participate in a joint research programme together with the Forschungszentrum Jülich.

References

- 1 A. J. Moulson, *Electroceramics, Materials, Properties and Applications*, Chapman and Hall, New York, USA (1990).
- 2 B. Huybrechts, K. Ishizaki and M. Takakata, *J. Mat. Sci.*, 1995, **30**, 2463.
- 3 E. Andrich, *Electr. Appl.*, 1965/1966, **26**, 123.
- 4 E. Andrich, *Philips Techn. Rev.*, 1969, **30**, 119.
- 5 K. Mihara and H. Niimi, *US-patent 7.075.408 B2* (2006).
- 6 W. Heywang, *Solid-State Electron.*, 1961, **3**, 51.
- 7 G. H. Jonker, *Solid-State Electron.*, 1964, **7**, 895.
- 8 G. Goodman, *J. Am. Ceram. Soc.*, 1963, **43**, 48.
- 9 J. Daniels and R. Wernicke, *Philips Res. Rep.*, 1976, **31**, 544.
- 10 J. Daniels and R. Wernicke, *Philips Res. Rep.*, 1976, **31**, 489.
- 11 D. Hennings, *Philips Res. Rep.*, 1976, **31**, 516.
- 12 H. Niimi, T. Ishikawa, K. Mihara, Y. Sakabe and M. Kuwabara, *Jap. J. Appl. Phys.*, 2007, **46**, 675.
- 13 Y.H. Hu, M.P. Harmer and D.M. Smyth, *J. Am. Ceram. Soc.*, 1985, **68**, 372.
- 14 S. Lee, C. Randall and Z.-K. Liu, *J. Am. Ceram. Soc.*, 2007, **90**, 2589.
- 15 S. Lee, C. Randall and Z.-K. Liu, *J. Am. Ceram. Soc.*, 2008, **91**, 1753.
- 16 H.-G. Yeo, M.-H. Kuk, M.-H. Kim, T.-K. Song, D.-S. Bae, T.-G. Park, S.-I. Lee and C. Randall, *J. Kor. Ceram. Soc.*, 2005, **42**, 308.
- 17 D.E. Rase and R. Roy, *J. Am. Ceram. Soc.*, 1955, **38**, 389.
- 18 K.H. Felgner, T. Müller, H.T. Langhammer and H.-P. Abicht, *J. Eur. Ceram. Soc.*, 2001, **21**, 1657.
- 19 K. Szot, C. Freiburg and M. Pawelczyk, *Appl. Phys. A*, 1991, **53**, 563.
- 20 F. A. Kröger and H. J. Vink, *Solid State Physics* **3**, ed. F. Seitz and D. Turnbull, Academic Press, New York (1956) 307.
- 21 H. Katsu, Ph.D. thesis, RWTH-Aachen, ISBN 978-3-89336-741-2 (2011).
- 22 R. Moos and K.H. Härdtl, *J. Appl. Phys.*, 1996, **80**, 393.
- 23 N. H. Chan, R. K. Sharma and D. M. Smyth, *J. Am. Ceram. Soc.*, 1982, **65**, 372.
- 24 J. P. Straley, *J. Phys. D: Appl. Phys.*, 1981, **14**, 2101.
- 25 T. Kolodiaznyh, A. Petric, M. Niewczas, C. Bridges, A. Safa-Sefat and J. E. Greedan, *Phys. Rev. B*, 2003, **68**, 134110.
- 26 S. Lee, G. Yang, R. H. T. Wilke, S. Trolrier-Mc Kinstry and C. A. Randall, *Phys. Rev. B*, 2009, **79**, 085205.
- 27 H.-I. Yoo, S. W. Lee and C. E. Lee, *J. Electroceram.*, 2003, **10**, 215.
- 28 J. Itoh, D.-C. Park, N. Ohashi, I. Sakaguchi, I. Yamahima, H. Haneda and J. Tanaka, *Jap. J. Appl. Phys.*, 2002, **41**, 3798.
- 29 S. Shirasaki, M. Tsukioka, H. Yamamura, H. Oshima and K. Kakegawa, *Solid State Commun.*, 1976, **19**, 21.
- 30 S. Shirasaki, H. Yamamura, H. Haneda, K. Kakegawa and J. Moori, *J. Chem. Phys.*, 1980, **73**, 4640.
- 31 S. Shirasaki, H. Haneda, K. Arai and M. Fujimoto, *J. Mater. Sci.*, 1987, **22**, 4439.
- 32 R. D. Shannon, *Acta Cryst. A*, 1976, **32**, 751.
- 33 N. H. Chan and D. M. Smyth, *J. Am. Ceram. Soc.*, 1984, **67**, 286.
- 34 D. M. Smyth, *The Defect Chemistry of Metal Oxides*, Oxford University Press, Oxford, UK (2000).
- 35 N. H. Chan, R. K. Sharma and D. M. Smyth, *J. Am. Ceram. Soc.*, 1982, **65**, 167.
- 36 S. Lee, C. Randall and Z.-K. Liu, *J. Am. Ceram. Soc.*, 2009, **92**, 222.
- 37 Y. H. Hu, M. P. Harmer and D. M. Smith, *J. Am. Ceram. Soc.*, 1985, **68**, 372.
- 38 J. F. Ihlefeld, P. R. Daniels, S. M. Aygün, W. J. Borland and J.-P. Maria, *J. Mater. Res.*, 2010, **25**, 1064.
- 39 R. Wernicke, *phys. stat. sol. (a)*, 1978, **47**, 139.
- 40 R. Waser, T. Baiatu and K. H. Härtl, *J. Am. Ceram. Soc.*, 1990, **73**, 1645.